IEEE Photonics Journal
An IEEE Photonics Society Publication

Polarization and Time-Resolved Dynamics of a 1550-nm VCSEL Subject to Orthogonally Polarized Optical Injection

Volume 3, Number 3, June 2011

Kevin Schires
Antonio Hurtado
Ian D. Henning
Michael J. Adams

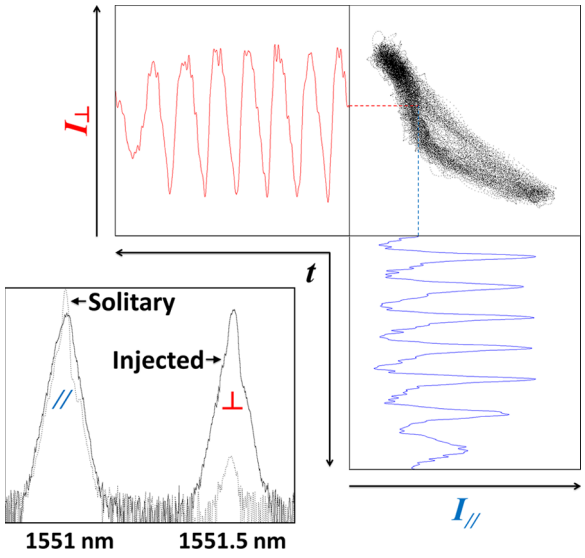

DOI: 10.1109/JPHOT.2011.2158636
1943-0655/$26.00 ©2011 IEEE

Polarization and Time-Resolved Dynamics of a 1550-nm VCSEL Subject to Orthogonally Polarized Optical Injection

Kevin Schires, Antonio Hurtado, Ian D. Henning, and Michael J. Adams

School of Computer Science and Electronic Engineering, University of Essex, CO4 3SQ, Colchester, U.K.

DOI: 10.1109/JPHOT.2011.2158636
1943-0655/$26.00 ©2011 IEEE

Manuscript received April 13, 2011; revised May 16, 2011; accepted May 16, 2011. Date of current version June 21, 2011. This work was supported in part by the U.K. Engineering and Physical Science Research Council under project EP/G012458/1 and by the European Commission under the Program FP7 Marie Curie Intra-European Fellowships Grant PIEF-GA-2008-219682. Corresponding author: K. Schires (e-mail: krschi@essex.ac.uk).

Abstract: We report a first experimental study of the simultaneous temporal and polarization-resolved dynamics of a 1550-nm vertical-cavity surface-emitting laser (VCSEL) subject to orthogonally polarized optical injection. A novel technique is used to reveal the behavior of both polarizations at the VCSEL's output. In general, the same type of dynamics can be seen in both polarizations of the fundamental transverse mode but with unequal intensity/modulation depth. We show that both polarizations exhibit period one and chaotic dynamics and reveal antiphase dynamics. These results offer promise for the development of dual-channel, anticorrelated periodic and chaotic-signal generators with a single VCSEL for use as oscillators or chaotic sources in present and future optical networks.

Index Terms: Vertical cavity surface emitting laser (VCSEL), nonlinear dynamical systems.

1. Introduction

A semiconductor laser under external optical injection can exhibit a wide range of nonlinear dynamics (see, for instance, [1] and [2] for reviews). There have been many reports analyzing these dynamics in different laser structures, including edge-emitting devices such as Fabry–Perot [3] or distributed feedback (DFB) [4] lasers but in multisection lasers as well [5] and, more recently, in vertical-cavity surface-emitting lasers (VCSELs) [6], [7] (see also [1], [2], and references therein). Of these VCSELs are very promising devices due to their inherent advantages such as on-wafer testing capability, reduced manufacturing costs, high-coupling efficiency to optical fibers, ease of integration in 2-D arrays, low threshold current, etc. (see, for instance, [8]). More specifically, optically injected long wavelength (LW) VCSELs emitting at 1550 nm are very promising devices for use as low-cost optical emitters for applications in optical networks from high-speed sources to optical switching/routing elements. In addition, enhanced modulation bandwidth, as well as reduced chirp and nonlinearities, have recently been reported in injection-locked 1550-nm VCSELs [9], [10]. Moreover, it is also known that optical injection into multimode lasers leads to complex dynamics between the different modes of the device [11]. Thus in the present contribution we focus on the analysis of polarization-resolved dynamics induced in a 1550-nm VCSEL subject to orthogonally polarized optical injection, whose optical spectrum exhibits two modes corresponding to the orthogonal polarizations of the fundamental transverse mode.

Considerable research effort has been dedicated in recent years to the topic of polarized optical injection in short wavelength (SW) [6], [12]–[16] and LW-VCSELs [7], [17]–[23], and different phenomena, such as polarization switching and bistability [12]–[14], [18]–[20], injection locking and nonlinear dynamics [15]–[17], [21]–[23], have been described. However the effect of polarized injection on the stability properties and nonlinear dynamics of both SW- and LW-VCSELs has yet to receive as much attention. Buesa *et al.* [6] reported a measured stability map based on the analysis of optical spectra for an 845-nm VCSEL subject to orthogonal optical injection. However, no further studies have been published for LW devices until recently, when we reported the first stability maps for 1550-nm VCSELs subject to parallel and orthogonally polarized injection, revealing the occurrence of differences in the stable locking range and regions of distinct nonlinear dynamics with applied bias current and different polarized injection [7], [21]–[23]. All these previous experimental studies mainly focused on the analysis of time-averaged spectra, using the so-called spectral signature method, where each different type of dynamics has a characteristic optical and electrical spectrum. However, although useful, the spectral signature method itself cannot provide a complete picture of the nonlinear dynamics as it averages the signals in time and, hence, eliminates important temporal information.

The direct analysis of real-time traces is therefore necessary to provide a complete picture of the nature of the nonlinear dynamics appearing in an optically injected laser. The availability of high performance real-time oscilloscopes has thus, in recent years, led to various experimental studies of the time-evolution of nonlinear dynamics in optically injected lasers. Valling *et al.* [24]–[26] proposed the study of time series of an optically injected solid-state laser and compared numerical solutions of the laser rate equations with experimental data. Using semiconductor lasers, Toomey *et al.* [27] have reported a real-time series analysis of the dynamics induced in a Fabry–Perot laser under optical feedback and modulation. Also, experimentally captured real-time series have been used to analyze excitability and dynamics in optically injected quantum-dot edge emitting devices [28]–[30] and very recently Kelleher *et al.* [31] have used real-time traces to contrast the excitability occurring in a quantum dot and a quantum-well (QW) device. In VCSELs, some previous studies have reported experimentally the use of time series to analyze the anticorrelated dynamics induced by optical feedback in SW emitting devices [32], [33]. However, we are not aware of any previous experimental studies analyzing real-time series for an optically injected LW-VCSEL. Furthermore, with the exception of a recent conference presentation [34] reporting measured averaged electrical spectra, we are not aware of any previous studies on optically injected LW-VCSEL that analyze simultaneously the dynamics induced in the two orthogonal polarizations of the fundamental transverse mode. Thus, in this paper, we report for the first time, to the best of our knowledge, a complete experimental study of the polarization-resolved dynamics of a 1550-nm VCSEL subject to orthogonally polarized optical injection. A novel technique based on the analysis of the experimentally measured real-time series captured simultaneously for both orthogonal polarizations of the fundamental mode of the 1550-nm VCSEL is used. The results obtained are compared to those measured when no polarization-resolved techniques are applied. This method provides new insights into the analysis of the dynamics induced in a 1550-nm VCSEL that could not be obtained otherwise by analyzing only the time-averaged optical and electrical spectra, as it includes a study of the temporal stability of dynamic states [35].

2. Experimental Setup

The experimental arrangement is shown in Fig. 1(a)–(c). Fig. 1(a) shows the part used to externally inject an orthogonally polarized optical signal into the 1550-nm VCSEL. A tunable master laser forms the external optical source and this is used in conjunction with a polarization controller to adjust the polarization relative to that of the lasing mode of the slave VCSEL. An optical attenuator is also included to vary the injection strength. A 85/15 coupler divides the optical input signal into two branches; the 85% port feeds directly into the slave laser (VCSEL) via an optical circulator, while the 15% port is connected to a power-meter for monitoring the injected optical power. The emitted signal from the VCSEL is separated using the circulator and passed through an erbium-doped fiber

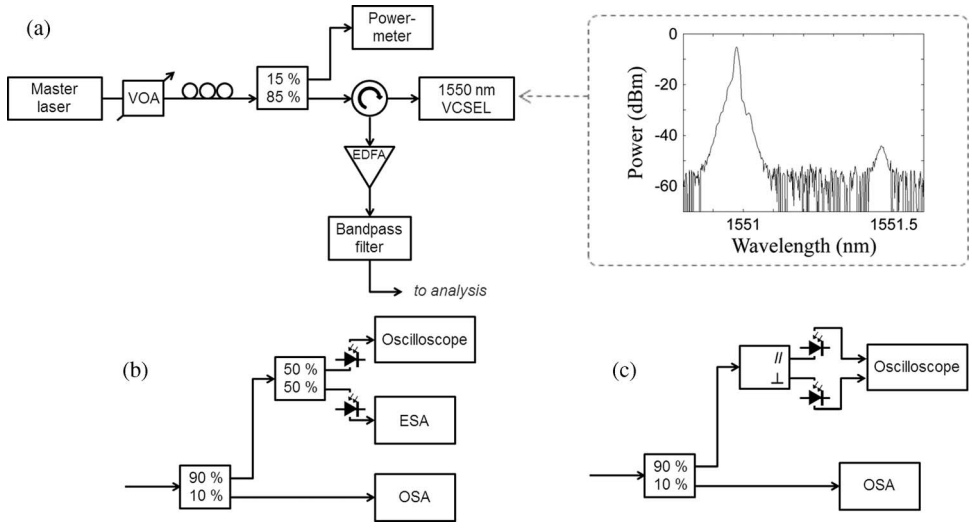

Fig. 1. (a) Setup used for the study of orthogonally polarized injection in a 1550-nm VCSEL. The spectrum of the VCSEL is given for a bias current of 5 mA (2.8 times above threshold). Two configurations are used for the analysis part of the setup: (b) for the analysis of the total signal and (c) for the simultaneous study of both polarizations.

amplifier (EDFA) to slightly boost the signal level to a few milliwatts balancing the signal-to-noise ratio while avoiding detector saturation. We also incorporate a narrow-band optical filter centered on the VCSEL's wavelength to remove the EDFA's broadband amplified spontaneous emission (ASE) noise prior to signal analysis. Two different signal analysis configurations were used. The first [see Fig. 1(b)] is used to study the total reflected signal, while the second configuration [see Fig. 1(c)] allows individual analysis of both orthogonal polarizations. The latter are separated using a polarization beam-splitter and are simultaneously monitored using an Agilent DSA91304A 13 GHz, four-channel real-time oscilloscope. Additional equipment also used in the experiments includes an optical spectrum analyzer (OSA) and an electrical spectrum analyzer (ESA). These are used to spectrally characterize the nonlinear dynamics in both the optical and electrical domains. Finally, two closely matched fast photodiodes (12 GHz bandwidth) were used to detect the optical signals for electrical analysis with the ESA or the oscilloscope. To support the simultaneous measurement of the two orthogonal polarizations of the VCSEL on separate channels of the oscilloscope, the delay between both channels was characterized using the modulated tunable laser to induce temporal features into both polarizations (which were not "dynamics"). These features were used as the references to align the two channels.

The slave laser was a commercially available InAlGaAs/InP QW 1550-nm VCSEL [36]. The device had a threshold current of 1.8 mA at 293 K. The optical spectrum of the device which appears in the inset in Fig. 1(a) exhibits two modes that correspond to the two orthogonal polarizations of the fundamental transverse mode separated by approximately 0.5 nm (60 GHz). The polarization of the main lasing [at -5 dBm in the spectrum shown in Fig. 1(a)] and that of the subsidiary mode (at -44 dBm) are referred to as parallel and orthogonal polarizations throughout this work.

3. Experimental Results

Combining the setup included in Fig. 1(a) with the analysis approach described in Fig. 1(c), real-time series of the intensities of the orthogonal (I_x) and parallel (I_y) polarizations at the output of the VCSEL were captured and recorded simultaneously. Fig. 2 shows measured time series and phase plots for the intensities of the parallel (I_y, blue) and orthogonal (I_x, red) polarizations for four different values of injection strength (K) and frequency detuning (Δf) selected based on previous

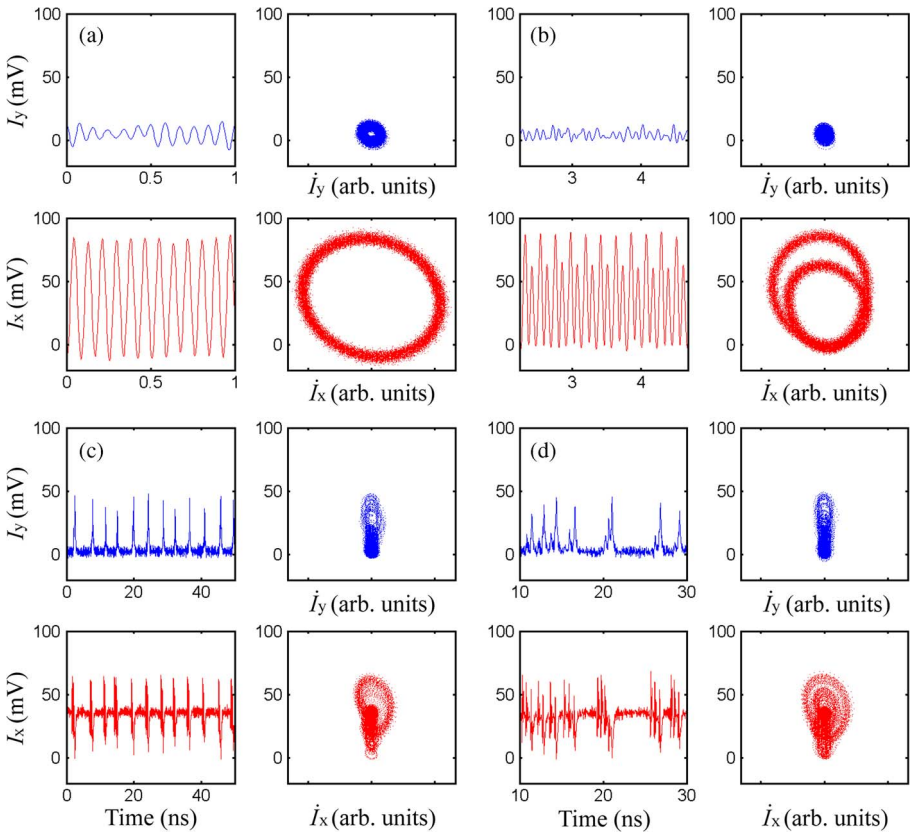

Fig. 2. Time series and phase plots of the parallel (I_y, blue) and orthogonal (I_x, red) polarizations. The VCSEL is biased five times above threshold and has a power of 615 μW. Phase plots are built plotting the time series against their derivative. K and Δf are (a) $\{1\ \text{dB}, 13.1\ \text{GHz}\}$, (b) $-\{3.2\ \text{dB}, 9.6\ \text{GHz}\}$, (c) $-\{14.1\ \text{dB}, 0.1\ \text{GHz}\}$, and (d) $-\{12.3\ \text{dB}, -0.9\ \text{GHz}\}$.

characterization of the dynamics [23], [37]. Phase plots are constructed by plotting the instantaneous signal intensity $I_{x,y}$ against its time derivative. The injection strength is defined as the injected power normalized to the power of the solitary VCSEL and the frequency detuning as the frequency difference between that of the externally injected signal and that of the resonance of the orthogonal polarization of the VCSEL. The VCSEL was biased five times above threshold to ensure that various strong dynamics can be found. Different types of nonlinear dynamic behaviors are found depending on the applied injection parameters. In particular, Fig. 2(a) shows the simultaneous occurrence of period one dynamics (P1, also referred as limit cycle) for both polarizations. In this case, as seen in Fig. 2(a), both time series exhibit periodic oscillations at a single frequency with both associated phase plots showing a characteristic open circular shape [1]. Additionally, the radius of the circle is indicative of the amplitude of the periodic oscillations. In contrast, Fig. 2(b) shows a different situation where period doubling (P2) dynamics occur for the orthogonal polarization (in red) whereas very small power fluctuations, almost hidden within the instrument's inherent noise background are observed for the output of the parallel polarization. In this latter case, the time series for the orthogonal polarization show oscillatory behavior at two different frequencies, the second frequency being half of the first, and the associated phase plot shows two distinct open circles [1]. Finally, Fig. 2(c) and (d) illustrate a completely different situation where chaotic dynamics with similar amplitudes are obtained simultaneously for the output of both polarizations. Strongly aperiodic behavior is observed in the measured time series, and the phase plots show a very irregular and poorly defined closed shape.

In Figs. 3 and 4, we compare the experimental nonlinear dynamics when measuring the total output signal of the VCSEL with those obtained when both orthogonal polarizations are analyzed

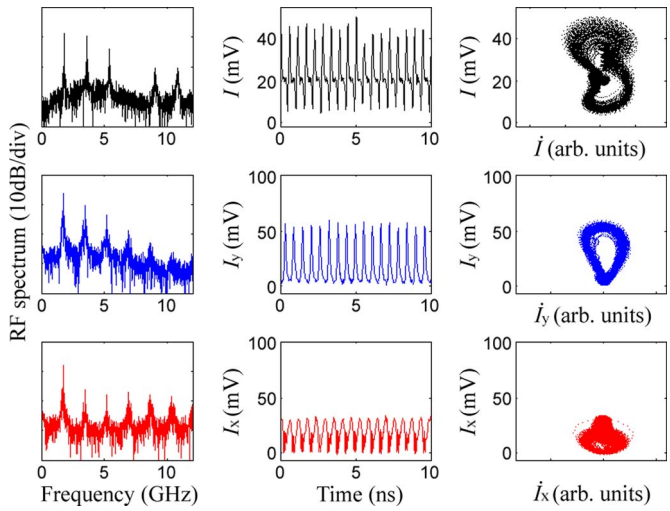

Fig. 3. Electrical Spectra (left), time series (center), and phase plots (right) of the total signal (black), parallel (blue), and orthogonal (red) polarizations of the VCSEL. $\{K = -10.5$ dB, $\Delta f = -3.6$ GHz$\}$. The VCSEL is biased 2.8 times above threshold and has a power of 330 μW.

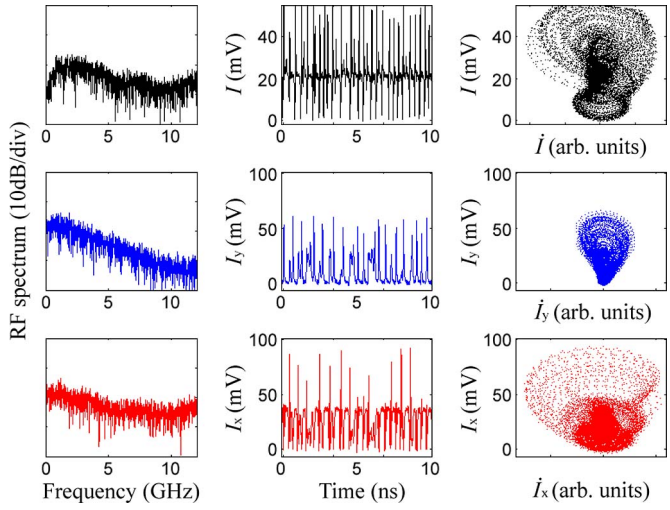

Fig. 4. Electrical Spectra (left), time series (center), and phase plots (right) of the total signal (black), parallel (blue), and orthogonal (red) polarizations of the VCSEL $\{K = -9.3$ dB, $\Delta f = -3.6$ GHz$\}$. The VCSEL is biased 2.8 times above threshold and has a power of 330 μW.

independently. In particular, we show electrical spectra, time series, and phase plots for the total output signal (black) and the orthogonal (blue) and parallel (red) polarizations for two different values of injection strength, i.e., $K = -10.5$ dB (see Fig. 3) and -9.3 dB (see Fig. 4), measured using the same detuning $\Delta f = -3.6$ GHz in both cases. It is important to note that all the time series in Figs. 3 and 4 and the associated phase plots are obtained from experimentally captured real-time signals. For comparison purposes, we also show the frequency spectra of the dynamics computed from the time series of the total output signal and each of the two individual polarizations obtained using a fast Fourier transform (FFT).

The frequency spectra in Fig. 3 suggest a situation where the total intensity exhibits dynamics with strong periodic components. However, the measured time series also reveals slower periodic variations in overall amplitude, with an envelope of periods of strong and weaker oscillation. This

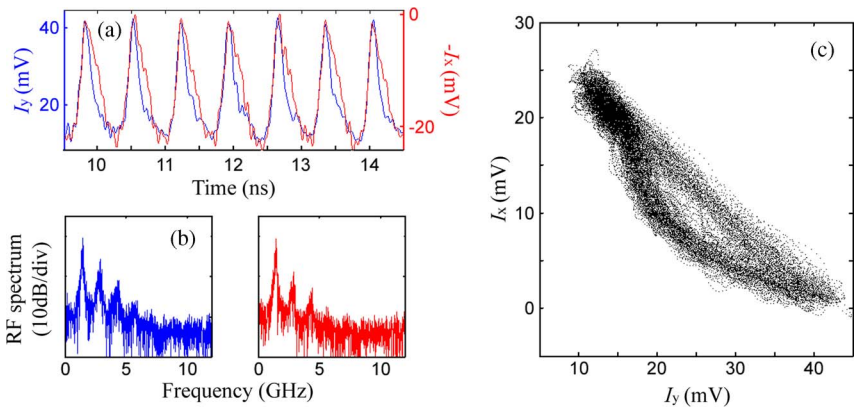

Fig. 5. (a) Real-time series of the parallel (blue) and orthogonal (red) polarizations intensities simultaneously measured at the VCSEL's output (for comparison purposes, a negative signed version of the orthogonal polarization intensity is included: −Ix). (b) Computed Electrical Spectra of the parallel (in blue) and orthogonal (in red) polarization output of the VCSEL, (c) Intensity of the parallel versus the orthogonal polarization (black). $\{K = -14.8$ dB, $\Delta f = -1.1$ GHz$\}$. The VCSEL is biased 2.8 times above threshold and has a power of 330 μW.

quasi-periodic behavior can be better seen from the phase plot (top row, right figure), which, despite being slightly spread in the top half of the phase plane, exhibits an open shape, which is characteristic of periodic dynamics [1]. Although noncircular in shape the degree of openness is indicative of quasi-periodic behavior with high amplitude oscillations.

Under the same measurement conditions, Fig. 3 also shows the time series, phase plots, and computed spectra for the two individual polarizations, i.e., orthogonal (middle row, in blue) and parallel (bottom row, in red), which exhibit very different behaviors. Their radio-frequency (RF) spectra calculated from the time series intensities are both characterized by the appearance of a very well defined harmonic structure with peaks spaced at the dominant oscillation frequency (approximately 1.8 GHz). Both polarizations seem to exhibit similar temporal characteristics but with different amplitudes and relative phase; the amplitude of the oscillations of the parallel polarization is higher than those of the orthogonal one, and the signals are not in antiphase. This simultaneous periodic oscillation for both polarizations has been previously predicted in early theoretical work [14]–[16]. The phase plots provide further confirmation of this behavior as they both show closed-loop shapes with different degrees of openness, each covering only one half of the phase plane. The openness of the parallel polarization (middle row, right figure, in blue) is indicative of high amplitude periodic oscillations. On the other hand the orthogonal polarization (bottom row, left figure, in red) appears more closed as the amplitude of the oscillations is more irregular but also smaller which make the representation in the phase plane more sensitive to measurement noise. Additionally, Fig. 4 shows a different situation where chaotic dynamics are measured for the total signal output of the VCSEL (upper plots, in black), as seen in the behavior of the measured time series, the fuzziness, and irregular shape of the phase plot, as well as the broadened measured spectra with much increased pedestal. In this case, the analysis of the individual polarizations, orthogonal (middle row, in blue), and parallel (bottom row, in red) also reveal that chaotic dynamics appear in both of them. Additionally, as seen in Fig. 3, some features of the time series of one of the polarizations are found mirrored in the other one. In this case, the amplitude of the oscillations in the orthogonal polarization is higher than those in the parallel. Finally, the similarity of the calculated RF spectra shows that the strong chaotic dynamics observed in the total output signal are a combination of those observed for both individual polarizations.

It is also interesting to note that under the right conditions both polarizations can exhibit antiphase dynamics. This is shown in Fig. 5 for the VCSEL subject to orthogonally polarized injection with initial detuning and injection strength equal to $\Delta f = -1.1$ GHz and $K = -14.8$ dB, respectively. Fig. 5(a) shows the time series of the intensities of the parallel and orthogonal polarizations plotted together. An inverted version of the orthogonal polarization intensity $(-I_x)$ is included for

comparison purposes. Fig. 5(a) reveals the simultaneous occurrence of periodic dynamics (P1) in both polarizations. The electrical spectra computed from the FFT of both time series is included in Fig. 5(b) and reveals the similarity of their harmonic content. These spectra both show a dominant oscillation frequency with additional peaks corresponding to harmonics at multiples of that frequency. Fig. 5(a) also shows that the periodic dynamics appearing for both polarizations are in antiphase, with the maxima of the amplitude of one polarization coinciding with the minima of the other one. It is important to note here that the analysis of the experimental time series uniquely reveals the antiphase nature of the occurring dynamics, as that information cannot be extracted from the analysis of time-averaged spectra alone. Finally, in Fig. 5(c), we use the time series to plot the instantaneous intensities of the parallel versus orthogonal mode. This verifies the antiphase nature of the dynamics showing an approximate linear response with a negative slope. It is also important to note that, although the dynamics for both polarizations are in antiphase, the temporal emission differs slightly in the shape of the "trailing edges," as shown in Fig. 5(a). Moreover, RF spectra also reveal that the power ratio between the different frequency components is different for both polarizations. Taken together, these explain the appearance of a small deviation in Fig. 5(c) from a "perfectly" linear plot. We obtain a good straight line from the "rising edges" when both dynamics are in antiphase and are of very similar shape, but we get a slightly curved line where signals exhibit a slightly different shape in their "trailing edges." Antiphase dynamics have been reported experimentally in optically injected edge-emitting multimode lasers [11]; in addition, anticorrelated dynamics have been reported in both modal polarizations of SW-VCSELs subject to optical feedback (see [32], [33], and references therein). For optically injected VCSELs, the possibility of antiphase (and in-phase) periodic dynamics in both orthogonal polarization modes has been predicted theoretically [14]–[16]. However, we are not aware of any experimental work confirming these predictions. Thus, in this work, we report, to the best of our knowledge, a first experimental observation of antiphase dynamics for both modal polarizations of a 1550-nm VCSEL subject to orthogonally polarized optical injection. This result offers promise for novel applications of these devices, including the development of dual-channel, anticorrelated periodic, and chaotic-signal generators for use in optical telecommunication networks.

Finally, very recently, we have reported a first theoretical stability analysis [23] of a 1550-nm VCSEL subject to different polarized injection. For this purpose, we have developed a novel extension of the well-established Spin Flip Model (SFM) [38], [39]. This can model the behavior of a VCSEL when subject to arbitrary polarized optical injection (parallel, orthogonal, or elliptically polarized) into either of the two polarizations of the fundamental transverse mode of the device. Our first results, consisting of numerically generated stability maps identifying the boundaries of the injection locking range and regions of different nonlinear dynamics in a 1550-nm VCSEL subject to orthogonally polarized injection show very good agreement with the experimental findings [23]. Building on these early promising results we plan to extend our theoretical analysis to simulate the time- and polarization-resolved dynamics of a 1550-nm VCSEL when subject to different polarized injection and compare the results with measurements. This is the subject of ongoing research and results will be reported elsewhere.

4. Conclusion

In conclusion, we report a first experimental study of the polarization-resolved dynamics of a 1550-nm VCSEL subject to orthogonally polarized injection based on the observation and analysis of real-time experimental measurements. This novel approach permits the effective identification of the dynamics appearing in both polarizations, and provides new perspectives on their suitability for use as periodic or chaotic-signal generators. For the former the same type of dynamics is observed for both polarizations, where one of the polarizations usually exhibits stronger dynamics than the other. However, for chaotic operation different dynamics are found simultaneously in both polarizations, each having comparable amplitudes. In addition antiphase dynamics have also been experimentally reported for the first time for both orthogonal polarizations at the output of a 1550-nm VCSEL. In particular, the fact that chaotic dynamics can be induced simultaneously in both polarizations of the

VCSEL's fundamental transverse mode offers promise for the development of dual-channel, anticorrelated chaotic-signal generators using a single commercially available 1550-nm VCSEL.

Acknowledgment

The authors would like to thank Agilent U.K. for lending them the real-time 13-GHz scope and N. Khan and R. Al-Seyab (Essex), as well as A. Valle and L. Pesquera (Instituto de Física de Cantabria, Santander, Spain) for fruitful discussions.

References

[1] S. Wieczorek, "The dynamical complexity of optically injected semiconductor lasers," *Phys. Rep.*, vol. 416, no. 1/2, pp. 1–128, Sep. 2005.
[2] M. J. Adams, A. Hurtado, D. Labukhin, and I. D. Henning, "Nonlinear semiconductor lasers and amplifiers for all-optical information processing," *Chaos*, vol. 20, no. 3, pp. 037102-1–037102-12, Sep. 2010.
[3] T. B. Simpson, J. M. Liu, K. F. Huang, and K. Tai, "Nonlinear dynamics induced by external optical injection in semiconductor lasers," *Quantum Semiclassical Opt.*, vol. 9, no. 5, pp. 765–785, Oct. 1997.
[4] T. B. Simpson, "Mapping the nonlinear dynamics of a distributed feedback semiconductor laser subject to external optical injection," *Opt. Commun.*, vol. 215, no. 1–3, pp. 135–151, Jan. 2003.
[5] T. Pérez, M. Radziunas, H.-J. Wünsche, C. R. Mirasso, and F. Henneberger, "Synchronization properties of two coupled multisection semiconductor lasers emitting chaotic light," *IEEE Photon. Technol. Lett.*, vol. 18, no. 20, pp. 2135–2137, Oct. 2006.
[6] J. Buesa, I. Gatare, K. Panajotov, H. Thienpont, and M. Sciamanna, "Mapping of the dynamics induced by orthogonal optical injection in vertical-cavity surface-emitting lasers," *IEEE J. Quantum Electron.*, vol. 42, no. 2, pp. 198–207, Feb. 2006.
[7] A. Hurtado, A. Quirce, A. Valle, L. Pesquera, and M. J. Adams, "Nonlinear dynamics induced by parallel and orthogonal optical injection in 1550 nm vertical-cavity surface-emitting lasers," *Opt. Exp.*, vol. 18, no. 9, pp. 9423–9428, Apr. 2010.
[8] F. Koyama, "Recent advances of VCSEL photonics," *J. Lightwave Technol.*, vol. 24, no. 12, pp. 4502–4513, Dec. 2006.
[9] C.-H. Hang, L. Chrostowski, and C. J. Chang-Hasnain, "Injection locking of VCSELs," *IEEE J. Sel. Topics Quantum Electron.*, vol. 9, no. 5, pp. 1386–1393, Sep./Oct. 2003.
[10] E. K. Lau, X. X. Zhao, H. K. Sung, D. Parekh, C. Chang-Hasnain, and M. C. Wu, "Strong optical injection-locked semiconductor lasers demonstrating > 100-GHz resonance frequencies and 80-GHz intrinsic bandwidths," *Opt. Exp.*, vol. 16, no. 9, pp. 6609–6618, Apr. 2008.
[11] S. Osborne, A. Amann, K. Buckley, G. Ryan, S. G. Hegarty, G. Huyet, and S. O'Brien, "Antiphase dynamics in a multimode semiconductor laser with optical injection," *Phys. Rev. A*, vol. 79, no. 2, p. 023834, Feb. 2009.
[12] Z. G. Pan, S. Jiang, M. Dagenais, R. A. Morgan, K. Kojima, M. T. Asom, and R. E. Leibenguth, "Optical injection induced polarisation bistability in vertical-cavity surface-emitting lasers," *Appl. Phys. Lett.*, vol. 63, no. 22, pp. 2999–3001, Nov. 1993.
[13] B. S. Ryvkin, K. Panajotov, E. A. Avrutin, I. Veretennicoff, and H. Thienpont, "Optical-injection-induced polarisation switching in polarisation-bistable vertical-cavity surface-emitting lasers," *J. Appl. Phys.*, vol. 96, no. 11, pp. 6002–6007, Dec. 2004.
[14] M. Sciamanna and K. Panajotov, "Route to polarisation switching induced by optical injection in vertical-cavity surface-emitting lasers," *Phys. Rev. A*, vol. 73, no. 2, p. 023811, Feb. 2006.
[15] I. Gatare, M. Sciamanna, M. Nizette, H. Thienpont, and K. Panajotov, "Mapping of two-polarisation-mode dynamics in vertical-cavity surface-emitting lasers with optical injection," *Phys. Rev. E*, vol. 80, no. 2, p. 026218, Aug. 2009.
[16] M. Nizette, M. Sciamanna, I. Gatare, H. Thienpont, and K. Panajotov, "Dynamics of vertical-cavity surface-emitting lasers with optical injection: A two-mode model approach," *J. Opt. Soc. Amer. B*, vol. 26, no. 8, pp. 1603–1613, Jul. 2009.
[17] L. Chrostowski, B. Faraji, W. Hofmann, M.-C. Amann, S. Wieczorek, and W. W. Chow, "40 GHz bandwidth and 64 GHz resonance frequency in injection-locked 1.55 μm VCSELs," *IEEE J. Sel. Topics Quantum Electron.*, vol. 13, no. 5, pp. 1200–1208, Sep./Oct. 2007.
[18] K. H. Jeong, K. H. Kim, S. H. Lee, M. H. Lee, B. S. Yoo, and K. A. Shore, "Optical injection-induced polarisation switching dynamics in 1.5 μm wavelength single-mode vertical-cavity surface-emitting lasers," *IEEE Photon. Technol. Lett.*, vol. 20, no. 10, pp. 779–781, May 2008.
[19] A. Hurtado, I. D. Henning, and M. J. Adams, "Two-wavelength switching with a 1550 nm VCSEL under single orthogonal optical injection," *IEEE J. Sel. Topics Quantum Electron.*, vol. 14, no. 3, pp. 911–917, May/Jun. 2008.
[20] A. Quirce, A. Valle, and L. Pesquera, "Very wide hysteresis cycles in 1550-nm VCSELs subject to orthogonal optical injection," *IEEE Photon. Technol. Lett.*, vol. 21, no. 17, pp. 1193–1195, Sep. 2009.
[21] A. Hurtado, D. Labukhin, I. D. Henning, and M. J. Adams, "Injection locking bandwidth in 1550-nm VCSELs subject to parallel and orthogonal optical injection," *IEEE J. Sel. Topics Quantum Electron.*, vol. 15, no. 3, pp. 585–593, May/Jun. 2009.
[22] N. Khan, K. Schires, A. Hurtado, I. D. Henning, and M. J. Adams, "Current-dependence of polarisation switching and locking in an optically injected 1550 nm VCSEL," *IET Optoelectron.,* 2011, DOI: 10.1049/iet-opt.2010.0061.
[23] R. Al-Seyab, K. Schires, N. Khan, A. Hurtado, I. D. Henning, and M. J. Adams, "Dynamics of polarized optical injection in 1550 nm VCSELs: Theory and experiments," *IEEE J. Sel. Topics Quantum Electron.*, 2011, DOI: 10.1109/JSTQE.2011.2138683.
[24] S. Valling, T. Fordell, and A. M. Lindberg, "Experimental and numerical intensity time series of an optically injected solid state laser," *Opt. Commun.*, vol. 254, no. 4–6, pp. 282–289, Oct. 2005.

[25] S. Valling, T. Fordell, and A. M. Lindberg, "Maps of the dynamics of an optically injected solid-state laser," *Phys. Rev. A*, vol. 72, no. 3, pp. 033810-1–033810-8, Sep. 2005.
[26] S. Valling, B. Krauskopf, T. Fordell, and A. M. Lindberg, "Experimental bifurcation diagram of a solid state laser with optical injection," *Opt. Commun.*, vol. 271, no. 2, pp. 532–542, Mar. 2007.
[27] J. P. Toomey, D. M. Kane, M. W. Lee, and K. A. Shore, "Nonlinear dynamics of semiconductor lasers with feedback and modulation," *Opt. Exp.*, vol. 18, no. 16, pp. 16 955–16 972, Aug. 2010.
[28] B. Kelleher, D. Goulding, B. Baselga Pascual, S. P. Hegarty, and G. Huyet, "Phasor plots in optical injection experiments," *Eur. Phys. J. D*, vol. 58, no. 2, pp. 175–179, Jun. 2010.
[29] B. Kelleher, D. Goulding, S. P. Hegarty, G. Huyet, D.-Y. Cong, A. Martinez, A. Lemaitre, A. Ramdane, M. Fischer, F. Gerschutz, and J. Koeth, "Excitable phase slips in an injection-locked single-mode quantum dot laser," *Opt. Lett.*, vol. 34, no. 4, pp. 440–442, Feb. 2009.
[30] D. Goulding, S. P. Hegarty, O. Rasskazov, S. Melnik, M. Hartnett, G. Greene, J. G. McInerney, D. Rachinskii, and G. Huyet, "Excitability in a quantum dot semiconductor laser with optical injection," *Phys. Rev. Lett.*, vol. 98, no. 15, p. 153903, Apr. 2007.
[31] B. Kelleher, C. Bonatto, G. Huyet, and S. P. Hegarty, "Excitability in optically injected semiconductor lasers: Contrasting quantum-well- and quantum-dot-based devices," *Phys. Rev. E*, vol. 83, no. 2, p. 026207, Feb. 2011.
[32] Y. Hong, J. Paul, P. S. Spencer, and K. A. Shore, "Bias-current dependence of anticorrelation polarisation dynamics in vertical-cavity surface-emitting lasers with long external cavity," *Appl. Phys. Lett.*, vol. 89, no. 8, pp. 081123-1–081123-3, Aug. 2006.
[33] Y. Hong, J. Paul, P. S. Spencer, and K. A. Shore, "Optical feedback dependence of anticorrelation polarisation dynamics in vertical-cavity surface-emitting lasers," *J. Opt. Soc. Amer. B*, vol. 23, no. 11, pp. 2285–2290, Nov. 2006.
[34] P. Perez, A. Quirce, L. Pesquera, and A. Valle, "Polarisation-resolved nonlinear dynamics induced by orthogonal optical injection in 1550 nm-vertical-cavity surface-emitting lasers," in *IEEE 22nd ISLC Tech. Dig.*, 2010, pp. 89–90.
[35] K. Schires, A. Hurtado, I. D. Henning, and M. J. Adams, "Investigation of the stability of microwave oscillations in an optically injected 1550 nm-VCSEL," in *Proc. CLEO*, Baltimore, MD, 2011.
[36] M.-R. Park, W.-S. Han, K.-H. Lee, S.-J. Park, and B.-S. Yoo, "All-monolithic 1.55 μm InAlGaAs/InP vertical cavity surface emitting lasers grown by metal organic chemical vapor deposition," *Jpn. J. Appl. Phys.*, vol. 45, pp. L8–L10, 2006.
[37] A. Hurtado, K. Schires, N. Khan, A. Quirce, A. Valle, L. Pesquera, I. D. Henning, and M. J. Adams, "Experimental stability maps of a 1550 nm-VCSEL subject to polarized optical injection," in *Proc. SPIE*, 2010, vol. 7597, p. 75971L.
[38] M. San Miguel, Q. Feng, and J. V. Moloney, "Light-polarisation dynamics in surface-emitting semiconductor-lasers," *Phys. Rev. A*, vol. 52, no. 2, pp. 1728–1739, Aug. 1995.
[39] J. Martin-Regalado, F. Prati, M. San Miguel, and N. B. Abraham, "Polarisation properties of vertical-cavity surface-emitting lasers," *IEEE J. Quantum Electron.*, vol. 33, no. 5, pp. 765–783, May 1997.